



Impacts of aerosols
on short-range
weather forecasts

S. R. Kolusu et al.

This discussion paper is/has been under review for the journal Atmospheric Chemistry and Physics (ACP). Please refer to the corresponding final paper in ACP if available.

Impacts of Amazonia biomass burning aerosols assessed from short-range weather forecasts

S. R. Kolusu¹, J. H. Marsham^{1,2}, J. Mulcahy³, B. Johnson³, C. Dunning³,
M. Bush³, and D. V. Spracklen¹

¹Institute for Climate and Atmospheric Science, water@leeds, School of Earth and Environment, Leeds, LS2 9JT, UK

²National Centre for Atmospheric Science, Leeds, UK

³Met Office, FitzRoy Road, Exeter, EX1 3PB, UK

Received: 24 June 2015 – Accepted: 25 June 2015 – Published: 10 July 2015

Correspondence to: S. R. Kolusu (s.kolusu@leeds.ac.uk)

Published by Copernicus Publications on behalf of the European Geosciences Union.

Title Page

Abstract

Introduction

Conclusions

References

Tables

Figures



Back

Close

Full Screen / Esc

Printer-friendly Version

Interactive Discussion



**Impacts of aerosols
on short-range
weather forecasts**

S. R. Kolusu et al.

Title Page

Abstract

Introduction

Conclusions

References

Tables

Figures



Back

Close

Full Screen / Esc

Printer-friendly Version

Interactive Discussion



ing the vertical profile of stability in the lower atmosphere. The localised changes in rainfall tend to average out to give a 5 % (0.06 mm day^{-1}) decrease in total precipitation over the Amazonian region (except on day 2 with prognostic BBA). The change in water budget from BBA is, however, dominated by decreased evapotranspiration from the reduced net surface fluxes (0.2 to 0.3 mm day^{-1}), since this term is larger than the corresponding changes in precipitation and water vapour convergence.

1 Introduction

Landscape fires and open biomass burning emit large quantities of trace gases and aerosol to the atmosphere, altering atmospheric composition and impacting weather and climate (Bowman et al., 2009). They are the largest source of carbonaceous aerosols to the atmosphere, contributing 65 % of global total organic carbon (OC) emissions and 25 % of global total black carbon (BC) emissions (Lamarque et al., 2010). Moreover, biomass burning contributes to various air pollutants that adversely affect human health (Marlier et al., 2013). Biomass burning aerosols (BBA) can significantly alter the energy balance of the atmosphere and the Earth's surface by directly absorbing and scattering solar radiation (Reid et al., 2005), and indirectly by changing the cloud properties, thus modulating the hydrological cycle (Ramanathan et al., 2001; Andreae and Rosenfeld, 2008). As a result, BBA affects sensible and latent heat fluxes in the lower atmosphere altering the temperature of the Earth's surface (Yu et al., 2002; Ichoku et al., 2003). The direct and indirect effects of BBA cause changes in the regional weather and climate via changes in the stability of the atmosphere, height of the boundary layer (BL), regional atmospheric circulation, cloud formation and precipitation (Kaufman and Koren, 2006; Rosenfeld et al., 2008). Despite such impacts on regional weather, most operational weather forecasts only include a climatological treatment of BBA. Here we explore the impact of prognostic BBA on short-term weather forecasts over Amazonia.

**Impacts of aerosols
on short-range
weather forecasts**

S. R. Kolusu et al.

Title Page

Abstract

Introduction

Conclusions

References

Tables

Figures



Back

Close

Full Screen / Esc

Printer-friendly Version

Interactive Discussion



The majority of fires worldwide occur in the tropical countries (Crutzen and Andreae, 1990; van der Werf et al., 2010) and the tropics play a particularly pivotal role in tropospheric chemistry (Crutzen and Zimmermann, 1991). Landscape fires occur due to both natural and anthropogenic activities, such as forest fires, agricultural crop residue burning and deliberate burning of savannah grasslands, and deforestation for agricultural purposes. South America accounts for an estimated 15 % of global fire emissions of carbon from landscape fires and open biomass burning (van der Werf et al., 2010), with regional hotspots of fire activity around the edges of Amazonia. The Amazon region experiences a large number of fires each dry season (August–October). Emissions of BBA from fires greatly increase regional aerosol concentrations (Martin et al., 2010), with dry season AOD of up to 4 observed at 550 nm using AERONET sun photometers (Artaxo et al., 2013). Such large concentrations of BBA with large AOD values may have substantial impacts on the regional radiative balance. Procopio et al. (2004) used observations during the dry season to estimate that Amazonian BBA caused a clear-sky radiative effect of -5 to -12 W m^{-2} at top-of-atmosphere (TOA) and -21 to -74 W m^{-2} at the surface. Furthermore, Sena et al. (2013) used a combination of MODIS and CERES data to estimate daily direct TOA radiative effects, which reached -30 W m^{-2} locally. Rosário et al. (2013) used a regional model to estimate a surface radiative effect of -55 W m^{-2} . Such changes in fluxes must affect Amazonian weather and a better understanding of this has potential benefits for improving weather and climate prediction.

Modelling studies have explored the impact of BBA on regional weather and climate. Zhang et al. (2008) studied the direct effect of BBA using the regional climate model RegCM3 and found that BBA can weaken regional circulation, cloudiness and perturb land–atmosphere interactions. Zhang et al. (2009) showed that BBA can impact the monsoon circulation weakening the South American monsoon circulation by increasing atmospheric stability. Using WRF-Chem model over South America, Wu et al. (2011) showed that BBA suppressed the diurnal amplitude of convection by about 11 %, decreasing clouds (consistent with Cook and Highwood, 2004) and precipitation in the

feedbacks using prognostic CLASSIC BBA scheme over South America. The paper is organized as follows; Data, model and methods are presented in Sect. 2. Section 3 presents results and discussion. Finally, summary and conclusions are presented in Sect. 4.

2 Model and data

2.1 Model

The MetUM (Davies et al., 2005) is used on a wide range of spatial and temporal scales from high-resolution short-range numerical weather prediction (NWP) to multi-decadal and centennial simulations in an earth system model configuration (Collins et al., 2011). In this study a limited area model (LAM) configuration of the MetUM is set up over Brazil (Fig. 1) with a horizontal grid spacing of 0.1° latitude/longitude (around 12 km) and 70 levels in the vertical (model lid at 80 km). Simulations are run covering the SAMBBA campaign period (14 September to 03 October 2012). Meteorological boundary conditions (3 hourly) are provided from the global operational NWP model. The atmospheric boundary layer is modelled following Brown et al. (2008) while convection is parameterized using the mass flux scheme based on Gregory and Rowntree (1990). Large-scale precipitation uses the single moment scheme based on Wilson and Ballard (1999), while large-scale cloud is parameterized using the scheme of Smith (1990). Cloud amount is diagnosed as a function of relative humidity by assuming the sub-grid humidity distribution follows a symmetric triangular function centred on the grid-box mean. The width of this distribution is reduced near the surface to account for the reduced variability expected with smaller volume grid-boxes on thinner near-surface model levels. The radiation scheme employed is the 2-stream radiation code of Edwards and Slingo (1996) with 6 and 9 bands in the shortwave (SW) and longwave (LW) parts of the spectrum respectively. The simulations are initialised using a continuous 6 hourly cycle of three-dimensional variational data assimilation (3-D-Var)

Impacts of aerosols on short-range weather forecasts

S. R. Kolusu et al.

Title Page

Abstract

Introduction

Conclusions

References

Tables

Figures



Back

Close

Full Screen / Esc

Printer-friendly Version

Interactive Discussion



Lorenc et al. (2000) with a 2 day forecast run daily at 00:00 UTC (20:00 (UTC – 4) local time in Porto Velho, Brazil).

Three model experiments, encompassing different representations of aerosols, were conducted to investigate the impact of BBA (Table 1). Firstly, a simulation without any aerosol representation (hereafter termed as NOA) is conducted. Secondly, a set of simulations which include monthly mean speciated aerosol climatologies (hereafter termed as CLIM). The climatologies are generated from HadGEM2 climate simulations using the CLASSIC (Coupled Large-scale Aerosol Simulator for studies in Climate) aerosol scheme (Bellouin et al., 2011). Aerosol species represented include sulphate, mineral dust, biomass burning, OC from fossil fuel, BC from fossil fuel, sea salt and nitrate aerosol. Due to the cost associated with running a fully coupled prognostic aerosol scheme operationally at high spatial resolution the global operational NWP configuration of the MetUM currently uses these monthly climatologies for all aerosol species apart from mineral dust. Finally, prognostic BBA is included using the BBA component of CLASSIC (hereafter named as PROG). In PROG aerosol climatologies are still used for all other aerosol species, i.e. other than BBA.

A full description of the CLASSIC BBA scheme is given in Bellouin et al. (2011). In PROG, daily BBA emissions are taken from the Global Fire Assimilation System (GFAS) version 1.1 emission dataset (Kaiser et al., 2012). These include global emission fluxes from open BB such as deforestation and crop residue burning estimated from satellite-based fire radiative power observations. A number of previous modelling studies have increased BBA emissions by up to a factor 5 to improve model agreement with observed AOD (Marlier et al., 2013; Ward et al., 2012; Tosca et al., 2013). Here, GFAS emissions were scaled by a factor of 1.7 to give improved agreement of modelled AOD against AERONET observations. In all simulations including an aerosol representation, the aerosols are coupled to the radiation scheme (which is called hourly) allowing the direct and semi-direct effect of the aerosols to be simulated. The aerosols do not affect assumed cloud droplet concentrations and so there is no representation of aerosol-cloud microphysical interactions, except for wash-out of BBA by rain in PROG.

Impacts of aerosols on short-range weather forecasts

S. R. Kolusu et al.

Title Page

Abstract

Introduction

Conclusions

References

Tables

Figures



Back

Close

Full Screen / Esc

Printer-friendly Version

Interactive Discussion



Impacts of aerosols on short-range weather forecasts

S. R. Kolusu et al.

Title Page

Abstract

Introduction

Conclusions

References

Tables

Figures



Back

Close

Full Screen / Esc

Printer-friendly Version

Interactive Discussion



et al. (2012) which showed a positive change for higher AODs (i.e. Earth–atmosphere warming), and the magnitude of the change in surface radiation is consistent with other studies (Procopio et al., 2004; Kaufman and Koren, 2006; Rosenfeld et al., 2008; Sena et al., 2013). The increase in radiative absorption across the atmosphere (ATM) is between around 10 and 20 W m⁻² (slightly greater in CLIM than PROG due to greater AODs) (Fig. 4c and f). The radiative absorption range by aerosols in the atmosphere found for whole period is in good agreement with the value of 18.7 W m⁻² found in a case study from the same period using the WRF-Chem model (which includes prognostic BBA with both direct and indirect effects from (Archer-Nicholls et al., 2015).

More subtle impacts on model cloud fields are found in PROG and CLIM on horizontal scales of a around one degree and a systematic decrease in high and medium cloud fraction of around 0.1 is found in areas of highest AODs (cloud changes are described later in Sect. 3.3). This may be a result of BBA stabilising the atmosphere, as discussed in Sects. 1 and 3.3. Changes in all-sky net radiation, which include the impacts of changes in the cloud fields resulting from BBA's direct effects, are lower in magnitude by around a factor of two compared with clear-sky values (Table 2), but the overall patterns are similar (not shown), i.e. the reduced cloud in PROG and CLIM compared with NOA decreases the magnitude of the surface and TOA cooling induced by the BBA.

3.3 Impacts of BBA on atmospheric thermodynamics

Over the whole SAMBBA period, the decrease in net surface radiation from BBA decreases the mean 2 m air temperatures by up to 1.4 °C, but with local increases of up to about 0.5 °C due to changes in cloud (Fig. 5). In PROG, the mean impact over Box A is a 0.1 °C decrease on day 1, reaching 0.2 °C decrease on day 2 (Table 2; effect is 0.03 °C larger in CLIM). The largest changes are found, as expected, close to regions of maximum BBA. The differences are largely restricted to the land, where air temperatures respond to the modelled surface energy balance. Tosca et al. (2010) showed that BBA can affect SSTs around Indonesia, but in all simulations here the SSTs are

prescribed from reanalysis. Over land, the BBA cools the surface skin temperature by approximately 0.2°C on day 1 and 0.3°C on day 2. Over Box A 10 m wind-speeds are reduced (Table 2), likely due to decreased surface sensible heat fluxes reducing downward mixing of momentum to the surface.

The impacts of BBA on atmospheric radiative and surface heating rates affects the thermodynamic structure of the atmosphere far above the surface. Figure 6a shows potential temperature cross sections averaged over the 10 to 13°S latitude belt, chosen as it is the region where surface impacts of BBA are largest in Figs. 4 and 5. Figure 6a and b are plotted for 18:00 UTC (14:00 local time) in order to show a well developed afternoon BL, with BL depth shown for NOA (white line) and PROG (red line). BBA mass concentrations (contoured) are well mixed within the BL and extend higher in the east where the BL is deeper (around 400 hPa, compared with 500 hPa in the west). Figure 6a shows that BBA cools the lower atmosphere over land (blue colours in Fig. 6a), consistent with the reduced net surface radiation. This cooling is deeper in the east where the BL is deeper (reaching around 700 hPa). BBA warms the atmosphere above this (red colours in Fig. 6a) with this warming centered around the top of the BL, or just above it. This warming is consistent with the direct radiative effects of the BBA, extending higher in the east where the BBA extends higher. The reduced net surface radiation from BBA reduces surface fluxes and this, combined with the increased atmospheric heating from BBA, reduces entrainment into the BL, and so BL depth reduces by up to 150 m (Fig. 6b) with a daily mean impact of 19 m over Box A (Table 2).

Figure 6 shows that the effects of BBA on temperatures above the surface layer are between -0.2 and $+0.2^{\circ}\text{C}$ when averaged over the entire SAMBBA period ($\sim \pm 0.4^{\circ}\text{C}$ in the first sub-period, with similar patterns, not shown). The effect of the BBA on temperature extend well above the BBA, with effects between 100 to 400 hPa as large as those lower in the atmosphere. Overall, there is a weak cooling at the surface and above the aerosol layer, and warming at 150 hPa (corresponding to approximately 15 km altitude). These changes are consistent with Chen et al. (2014) who simulated radiative effects during a wild fire event over the United States using WRF-Chem model.

Impacts of aerosols on short-range weather forecasts

S. R. Kolusu et al.

[Title Page](#)[Abstract](#)[Introduction](#)[Conclusions](#)[References](#)[Tables](#)[Figures](#)[Back](#)[Close](#)[Full Screen / Esc](#)[Printer-friendly Version](#)[Interactive Discussion](#)

These are also consistent with changes in vertical motion induced by the BBA, as discussed below.

Cross-sections of relative humidity (RH), ice cloud water (QCF), liquid cloud water (QCL) are presented in Fig. 7 at 18:00 UTC, in a similar manner to Fig. 6a for potential temperature. Differences in the RH profiles are consistent with changes in the potential temperature profile within the BL. BBA tends to decrease RH above the BL (Fig. 7a), consistent with the warming induced there (Fig. 6a), although differences in the patterns shown in Figs. 6a and 7 show that changes in water vapour mixing ratio (WVMR) are also important for RH. Consistent with the decrease in RH from BBA above the BL, BBA decreases both QCF and QCL (Fig. 7b, and c), i.e BBA suppresses middle and high level clouds, consistent with aerosol semi-direct effects from other studies (Jacobson, 2002; Korontzi et al., 2004; Wu et al., 2011; Chen et al., 2014).

Figure 8a shows changes in geopotential and horizontal and vertical winds for the same cross-section as Fig. 6a. The surface cooling with heating above, induced by the BBA, which has a vertical extent that depends on the BL depth and height of the BBA, and an intensity that depends on the BBA loading, induces a weak surface high pressure around 50° W and a weak low pressure at 65° W (Fig. 8a). Low-level wind changes are consistent with this, but only reach 0.5 ms⁻¹. The effects are stronger at 700 hPa, where the horizontal gradient in BL depth and BBA heating gives a low pressure relative to NOA at around 50° W and a relative high pressure at 65° W. This gives a weak anti cyclonic circulation at this level in the runs with BBA compared with NOA (Fig. 8b), with differences in winds reaching 0.6 ms⁻¹.

Changes in winds above 400 hPa are again consistent with the changes in geopotential there, and are larger than below, due to the strong winds at this level in the atmosphere. Figure 8a shows that BBA generates ascent and so cooling centered at around 350 hPa and 65° W and descent above, consistent with the cooling and warming shown at these levels in Fig. 6a. Small changes in vertical winds (Fig. 8a white lines) cause relatively large changes in temperature at these heights in the atmosphere, which are very stable. The fact that the temperature changes at these levels are consistent with

Impacts of aerosols on short-range weather forecasts

S. R. Kolusu et al.

Title Page

Abstract

Introduction

Conclusions

References

Tables

Figures



Back

Close

Full Screen / Esc

Printer-friendly Version

Interactive Discussion



turnal stable layer, a common problem in regional NWP models. For temperature and humidity, differences between the aerosol simulations are generally small apart from at Boa Vista where PROG leads to an increase in relative humidity above 850 hPa. The model biases in temperature will affect vertical mixing of aerosol, but we do not anticipate that they substantially affect modelled sensitivities to BBA.

3.5 Impacts of BBA on precipitation and the water budget

Although the simulations conducted in this study do not couple the BBA with cloud microphysical processes, the BBA can alter precipitation as direct radiative effects have an impact on clouds and convection. Figure 11a shows the mean precipitation rate averaged over the whole campaign for the NOA simulation. There are large local differences in mean rainfall between the three simulations (NOA, PROG, CLIM) (Fig. 11b and c), mainly due to changes in the location of precipitation events. When smoothed over a 150 km grid these changes are still around 4 mm day^{-1} , although the change in the regional mean is small: for Box A (Fig. 11a), BBA in PROG or CLIM reduces rain by around $0.055 \text{ mm day}^{-1}$ compared with NOA (mean rainfall is 1.2 mm day^{-1}). Precipitation reductions of $\sim 5\%$ found in this study are therefore slightly greater than the Tosca et al. (2013) study which shows a (2%) decrease over Amazonia.

Changes in the pdf of rainfall over Box A are shown in Fig. 11d and e, with absolute changes in the pdf shown in grey and fractional changes in blue. For both PROG and CLIM, BBA tends to increase the frequency of both no rainfall and the highest rainfall rates, while decreasing moderate rainfall rates. A Kolmogorov–Smirnov test conducted for the samples showed that the results are statistically significant at 98% confidence level. This effect on rain-rates may be linked to BBA increasing stability in the lower atmosphere, due to reduced net surface flux and increased radiative warming of the atmosphere.

To further explore the mechanisms for simulated changes in rainfall we calculated the water budget over Box A for all model simulations on day 1 and day 2. BBA reduces the net radiation, this causes a decrease in surface evapotranspiration (0.2 and

Impacts of aerosols on short-range weather forecasts

S. R. Kolusu et al.

Title Page	
Abstract	Introduction
Conclusions	References
Tables	Figures
◀	▶
◀	▶
Back	Close
Full Screen / Esc	
Printer-friendly Version	
Interactive Discussion	



Impacts of aerosols on short-range weather forecasts

S. R. Kolusu et al.

Title Page

Abstract

Introduction

Conclusions

References

Tables

Figures



Back

Close

Full Screen / Esc

Printer-friendly Version

Interactive Discussion



0.3 mm day⁻¹ in PROG and CLIM, a 5 and 6% decrease respectively, Table 2). The radiative heating from the BBA enhances the stability of the atmosphere generally reduces precipitation by 0.05 to 0.12 mm day⁻¹, except in day 2 of PROG which shows a small (0.02 mm day⁻¹) increase. The change in water vapour convergence into box A is unclear with small increases and decreases in PROG and CLIM for days 1 and 2 (−0.02 to +0.1 mm day⁻¹). The overall consequence is that the change in water budget of box A from BBA is dominated by the reduction in surface evapotranspiration resulting from the decreased net surface radiation. Therefore, the overall net effect of BBA is a drying of the atmosphere in the Amazonian region, largely due to reduced latent heat fluxes. The drying of the atmosphere due to BBA will be further investigated in future studies using the United Kingdom Chemistry and Aerosol (UKCA) model, including indirect radiative effects.

4 Summary and conclusions

A limited area version of the Met Office Unified Model (MetUM) is used to investigate direct radiative effects of biomass burning aerosol (BBA) over tropical South America during the end of the dry season (the SAMBBA period of 14 September to 03 October 2012) and impacts on the atmosphere and short-range weather forecasts. Three simulations were conducted with different aerosols representations: (i) no aerosols (NOA), (ii) monthly mean climatology BBA (CLIM), (iii) BBA modelled prognostically with the CLASSIC aerosol scheme (PROG). Impacts are quantified from the first 2 days of forecasts initialised from meteorological analyses.

The modelled BBA reduced clear-sky net radiation at the TOA by 8 W m⁻² over the region studied and reduced clear-sky net radiation at the surface by on average of 15 W m⁻², with direct warming of the atmosphere due to absorption of solar radiation of 7 W m⁻². BBA reduced cloud cover and all-sky radiative effects were lower than clear-sky effects: −4 and −9 W m⁻² for the TOA and surface net radiative effects, respectively. The reduced net surface radiation from BBA cooled the mean 2 m air temperature by

on average 0.1 °C. The temperature changes found here are less than the ~ -0.3 °C changes found by Wu et al. (2011) using WRF–Chem model over the South America during the dry period of September 2011. This difference in results is consistent with the higher AODs in the Wu et al. (2011) study.

The BBA cools the lower BL by around 0.2 °C, but heats the atmosphere above by up to 0.2 °C in the elevated BBA layer that extend to between 600 and 400 hPa. The cooling of the BL is consistent with the BBA reducing surface sensible heat fluxes. This reduces BL growth and results in a decrease in the mean BL depth by around 19 m. The BBA induces a weak (0.2 ms^{-1}) cyclonic circulation in the lower BL, with a weak anticyclonic circulation above (up to 0.6 ms^{-1}) due to the horizontal gradients in BBA heating. Effects of BBA are communicated to the upper troposphere due to changes in uplift and subsidence affecting mean upper tropospheric temperatures by up to +0.2 °C.

The evaluation against observations shows that the model simulations that included aerosols gave a better representation of near-surface air temperature and relative humidity than models without aerosols (mean correlation of 0.79 and 0.72 in NOA compared to 0.83 and 0.79 in PROG for near surface air temperature and RH respectively with 99% significant confidence level). However, the improvements were small compared with model error. The difference in results between simulations with a climatological and prognostic representation of aerosols were even smaller and statistically insignificant. Similarly, comparison with radiosondes show negligible differences from including BBA compared with model error. These results suggest that while inclusion of a realistic representation of BBA has impacts on the model radiation fields, improvements on the mean forecast skill are small at the 2 day forecast lead times analysed in this study. This is most likely due to the strong constraint of the 3-D-VAR data assimilation at short forecast lead times. Indeed impacts on the meteorology on day 2 of the forecast were larger than on day 1 (Table 2) indicating that prognostic BBA might have larger impacts on longer medium to seasonal range weather forecast and on climate

Impacts of aerosols on short-range weather forecasts

S. R. Kolusu et al.

[Title Page](#)[Abstract](#)[Introduction](#)[Conclusions](#)[References](#)[Tables](#)[Figures](#)[Back](#)[Close](#)[Full Screen / Esc](#)[Printer-friendly Version](#)[Interactive Discussion](#)

simulations. Future studies within SAMBBA will investigate this using individual case studies from the SAMBBA period.

The inclusion of a prognostic BBA scheme gives a superior aerosol forecast compared to an aerosol climatology, but in this study did not improve the mean model skill for temperature and relative humidity significantly over that of the BBA climatology. This reiterates the findings of Mulcahy et al. (2014) that the inclusion of realistic aerosol-radiative interactions are of key importance in operational NWP forecasting systems, but that in many cases a monthly varying speciated aerosol climatology can provide sufficient skill. However, given the highly variable nature of BB emissions the more advanced fully prognostic treatment of BBA is required in order to provide an accurate aerosol prediction capability.

In this study PROG and CLIM BBA tended to reduce mean precipitation by around 5% (0.06 mm day^{-1} , Table 2), although PROG gave a small increase on day 2 (0.02 mm day^{-1}). It can be speculated that such reductions may lead to more biomass burning over Amazonia (Aragao et al., 2014). However, it should be noted that aerosol-cloud feedbacks on cloud brightness, lifetime and precipitation efficiency, which may alter the sensitivity of precipitation to BBA, were not modelled in this study. The BBA also led to changes in the location of convection, resulting in localised changes in precipitation of around 4 mm day^{-1} , when smoothed on a 150 km scale. Furthermore, the BBA decreased the frequency of moderate rain rates, and increased the frequency of both no rain and high rain rates. These changes in the distribution of rainfall intensity may be linked to the stabilisation of the lower atmosphere by BBA through the direct radiative effects.

The water vapour budget analysis over the Amazonian region reveals that by reducing the net surface radiation, the BBA reduces surface latent heat fluxes by 0.2 mm day^{-1} . There is a drying of the atmosphere as this reduction in latent heat fluxes is not compensated by the reduced precipitation (around $-0.06 \text{ mm day}^{-1}$), or increased water vapour convergence (-0.02 to $+0.1 \text{ mm day}^{-1}$). Such impacts of BBA on the water budget of Amazonia will be investigated in future SAMBBA modelling

Impacts of aerosols on short-range weather forecasts

S. R. Kolusu et al.

Title Page

Abstract

Introduction

Conclusions

References

Tables

Figures



Back

Close

Full Screen / Esc

Printer-friendly Version

Interactive Discussion



studies using longer simulations that are more free to evolve away from their initial state.

Acknowledgements. The MODIS data used in this study were produced with the Giovanni online data system, developed and maintained by the National Aeronautics and Space Administration (NASA) GES DISC. We acknowledge the MODIS teams for the data used. We thank Jim Haywood for a careful reading and discussion of the manuscript. We thank the Principal investigators and their staff for establishing and maintaining the 8 AERONET sites used in this investigation. The Facility for Airborne Atmospheric Measurement (FAAM) BAe-146 Atmospheric Research Aircraft is jointly funded by the Met Office and Natural Environment Research Council (NERC) and operated by DirectFlight Ltd. We would like to the dedicated efforts of FAAM, DirectFlight, the National Institute for Space Research (INPE), University of Sao Paulo, and the Brazilian Ministry of Science and Technology in making the SAMBBA measurement campaign possible. We thank to Joel Brito from University of Sao Paulo for providing surface observation over the Amazonia state. The SAMBBA project was funded by the Met Office and NERC with grant number NE/J009822/1. We acknowledge use of the MONSooN system, a collaborative facility supplied under the Joint Weather and Climate Research Programme, which is a strategic partnership between the Met Office and NERC.

References

- Andreae, M. and Rosenfeld, D.: Aerosol–cloud–precipitation interactions. Part 1. The nature and sources of cloud-active aerosols, *Earth-Sci. Rev.*, 89, 13–41, 2008. 18885
- Aragao, L. E., Poulter, B., Barlow, J. B., Anderson, L. O., Malhi, Y., Saatchi, S., Phillips, O. L., and Gloor, E.: Environmental change and the carbon balance of Amazonian forests, *Biol. Rev.*, 89, 913–931, 2014. 18900
- Archer-Nicholls, S., Lowe, D., Schultz, D. M., and McFiggans, G.: Aerosol-radiation-cloud interactions in a regional coupled model: a comparison of the effects of convective parameterisation and resolution, in preparation, 2015. 18893
- Artaxo, P., Rizzo, L. V., Brito, J. F., Barbosa, H. M., Arana, A., Sena, E. T., Cirino, G. G., Bastos, W., Martin, S. T., and Andreae, M. O.: Atmospheric aerosols in Amazonia and land use change: from natural biogenic to biomass burning conditions, *Faraday Discuss.*, 165, 203–235, 2013. 18886

Impacts of aerosols on short-range weather forecasts

S. R. Kolusu et al.

Title Page

Abstract

Introduction

Conclusions

References

Tables

Figures



Back

Close

Full Screen / Esc

Printer-friendly Version

Interactive Discussion



Impacts of aerosols on short-range weather forecasts

S. R. Kolusu et al.

Title Page

Abstract

Introduction

Conclusions

References

Tables

Figures



Back

Close

Full Screen / Esc

Printer-friendly Version

Interactive Discussion



versity of Manchester and the Met Office, available on request from the authors, 1–180, 2013. 18891

Davies, T., Cullen, M., Malcolm, A., Mawson, M., Staniforth, A., White, A., and Wood, N.: A new dynamical core for the Met Office's global and regional modelling of the atmosphere, Q. J. Roy. Meteor. Soc., 131, 1759–1782, 2005. 18888

Edwards, J. and Slingo, A.: Studies with a flexible new radiation code. I: Choosing a configuration for a large-scale model, Q. J. Roy. Meteor. Soc., 122, 689–719, 1996. 18888

Gregory, D. and Rowntree, P.: A mass flux convection scheme with representation of cloud ensemble characteristics and stability-dependent closure, Mon. Weather Rev., 118, 1483–1506, 1990. 18888

Haywood, J. and Boucher, O.: Estimates of the direct and indirect radiative forcing due to tropospheric aerosols: a review, Reviews of Geophysics-Richmond Virginia then Washington, 38, 513–543, 2000. 18892

Hoerger, M.: ZH: an updated version of Steiger's Z and web-based calculator for testing the statistical significance of the difference between dependent correlations, retrieved 1 March 2014, 2013. 18896

Holben, B. N., Eck, T. F., Slutsker, I., Tanré, D., Buis, J. P., Setzer, A., Vermote, E., Reagan, J. A., Kaufman, Y. J., Nakajima, T., Lavenu, F., Jankowiak, I., and Smirnov, A.: AERONET – a federated instrument network and data archive for aerosol characterization, Remote Sens. Environ., 66, 1–16, 1998. 18890

Ichoku, C., Remer, L. A., Kaufman, Y. J., Levy, R., Chu, D. A., Tanré, D., and Holben, B. N.: MODIS observation of aerosols and estimation of aerosol radiative forcing over southern Africa during SAFARI 2000, J. Geophys. Res.-Atmos., 108, 8499, doi:10.1029/2002JD002366, 2003. 18885

Ichoku, C., Remer, L. A., and Eck, T. F.: Quantitative evaluation and intercomparison of morning and afternoon Moderate Resolution Imaging Spectroradiometer (MODIS) aerosol measurements from Terra and Aqua, J. Geophys. Res.-Atmos., 110, D10S03, doi:10.1029/2004JD004987, 2005. 18890

Jacobson, M. Z.: Control of fossil-fuel particulate black carbon and organic matter, possibly the most effective method of slowing global warming, J. Geophys. Res.-Atmos., 107, 4410, doi:10.1029/2001JD001376, 2002. 18895

Kaiser, J. W., Heil, A., Andreae, M. O., Benedetti, A., Chubarova, N., Jones, L., Morcrette, J.-J., Razinger, M., Schultz, M. G., Suttie, M., and van der Werf, G. R.: Biomass burning emissions

Impacts of aerosols on short-range weather forecasts

S. R. Kolusu et al.

Title Page

Abstract

Introduction

Conclusions

References

Tables

Figures



Back

Close

Full Screen / Esc

Printer-friendly Version

Interactive Discussion



estimated with a global fire assimilation system based on observed fire radiative power, Biogeosciences, 9, 527–554, doi:10.5194/bg-9-527-2012, 2012. 18889

Kaufman, Y. J. and Koren, I.: Smoke and pollution aerosol effect on cloud cover, Science, 313, 655–658, 2006. 18885, 18893

5 King, M. D., Menzel, W. P., Kaufman, Y. J., Tanré, D., Gao, B.-C., Platnick, S., Ackerman, S. A., Remer, L. A., Pincus, R., and Hubanks, P. A.: Cloud and aerosol properties, precipitable water, and profiles of temperature and water vapor from MODIS, IEEE T. Geosci. Remote, 41, 442–458, 2003. 18890

10 Korontzi, S., Roy, D. P., Justice, C. O., and Ward, D. E.: Modeling and sensitivity analysis of fire emissions in southern Africa during SAFARI 2000, Remote Sens. Environ., 92, 376–396, 2004. 18895

15 Lamarque, J.-F., Bond, T. C., Eyring, V., Granier, C., Heil, A., Klimont, Z., Lee, D., Liousse, C., Mieville, A., Owen, B., Schultz, M. G., Shindell, D., Smith, S. J., Stehfest, E., Van Aardenne, J., Cooper, O. R., Kainuma, M., Mahowald, N., McConnell, J. R., Naik, V., Riahi, K., and van Vuuren, D. P.: Historical (1850–2000) gridded anthropogenic and biomass burning emissions of reactive gases and aerosols: methodology and application, Atmos. Chem. Phys., 10, 7017–7039, doi:10.5194/acp-10-7017-2010, 2010. 18885

20 Lorenc, A. C., Ballard, S. P., Bell, R. S., Ingleby, N. B., Andrews, P. L. F., Barker, D. M., Bray, J. R., Clayton, A. M., Dalby, T., Li, D., Payne, T. J., and Saunders, F. W.: The Met. Office global three-dimensional variational data assimilation scheme, Q. J. Roy. Meteor. Soc., 126, 2991–3012, 2000. 18889

Marlier, M. E., DeFries, R. S., Voulgarakis, A., Kinney, P. L., Randerson, J. T., Shindell, D. T., Chen, Y., and Faluvegi, G.: El Nino and health risks from landscape fire emissions in south-east Asia, Nature climate change, 3, 131–136, 2013. 18885, 18889

25 Martin, S. T., Andreae, M. O., Artaxo, P., Baumgardner, D., Chen, Q., Goldstein, A. H., Guenther, A., Heald, C. L., Mayol-Bracero, O. L., McMurry, P. H., Pauliquevis, T., Pöschl, U., Prather, K. A., Roberts, G. C., Saleska, S. R., Silva-Dias, M. A., Spracklen, D. V., Swietlicki, E., and Trebs, I.: Sources and properties of Amazonian aerosol particles, Rev. Geophys., 48, RG2002, doi:10.1029/2008RG000280, 2010. 18886

30 Mulcahy, J. P., Walters, D. N., Bellouin, N., and Milton, S. F.: Impacts of increasing the aerosol complexity in the Met Office global numerical weather prediction model, Atmos. Chem. Phys., 14, 4749–4778, doi:10.5194/acp-14-4749-2014, 2014. 18887, 18900

**Impacts of aerosols
on short-range
weather forecasts**

S. R. Kolusu et al.

Title Page

Abstract

Introduction

Conclusions

References

Tables

Figures



Back

Close

Full Screen / Esc

Printer-friendly Version

Interactive Discussion



Procopio, A., Artaxo, P., Kaufman, Y., Remer, L., Schafer, J., and Holben, B.: Multiyear analysis of Amazonian biomass burning smoke radiative forcing of climate, *Geophys. Res. Lett.*, 31, L03108, doi:10.1029/2003GL018646, 2004. 18886, 18892, 18893

Ramanathan, V., Crutzen, P., Kiehl, J., and Rosenfeld, D.: Aerosols, climate, and the hydrological cycle, *Science*, 294, 2119–2124, 2001. 18885

Reid, J. S., Eck, T. F., Christopher, S. A., Koppmann, R., Dubovik, O., Eleuterio, D. P., Holben, B. N., Reid, E. A., and Zhang, J.: A review of biomass burning emissions part III: intensive optical properties of biomass burning particles, *Atmos. Chem. Phys.*, 5, 827–849, doi:10.5194/acp-5-827-2005, 2005. 18885

Rosário, N. E., Longo, K. M., Freitas, S. R., Yamasoe, M. A., and Fonseca, R. M.: Modeling the South American regional smoke plume: aerosol optical depth variability and surface shortwave flux perturbation, *Atmos. Chem. Phys.*, 13, 2923–2938, doi:10.5194/acp-13-2923-2013, 2013. 18886

Rosenfeld, D., Lohmann, U., Raga, G. B., O'Dowd, C. D., Kulmala, M., Fuzzi, S., Reissell, A., and Andreae, M. O.: Flood or drought: how do aerosols affect precipitation?, *Science*, 321, 1309–1313, 2008. 18885, 18893

Sena, E. T., Artaxo, P., and Correia, A. L.: Spatial variability of the direct radiative forcing of biomass burning aerosols and the effects of land use change in Amazonia, *Atmos. Chem. Phys.*, 13, 1261–1275, doi:10.5194/acp-13-1261-2013, 2013. 18886, 18892, 18893

Simmons, A., Uppala, S., Dee, D., and Kobayashi, S.: ERA-interim: new ECMWF reanalysis products from 1989 onwards, *ECMWF Newsletter*, 110, 25–35, 2007. 18890

Smith, R.: A scheme for predicting layer clouds and their water content in a general circulation model, *Q. J. Roy. Meteor. Soc.*, 116, 435–460, 1990. 18888

Ten Hoeve, J. E., Jacobson, M. Z., and Remer, L. A.: Comparing results from a physical model with satellite and in situ observations to determine whether biomass burning aerosols over the Amazon brighten or burn off clouds, *J. Geophys. Res.-Atmos.*, 117, D08203, doi:10.1029/2011JD016856, 2012. 18892

Tosca, M. G., Randerson, J. T., Zender, C. S., Flanner, M. G., and Rasch, P. J.: Do biomass burning aerosols intensify drought in equatorial Asia during El Niño?, *Atmos. Chem. Phys.*, 10, 3515–3528, doi:10.5194/acp-10-3515-2010, 2010. 18893

Tosca, M. G., Randerson, J. T., and Zender, C. S.: Global impact of smoke aerosols from landscape fires on climate and the Hadley circulation, *Atmos. Chem. Phys.*, 13, 5227–5241, doi:10.5194/acp-13-5227-2013, 2013. 18887, 18889, 18897

Impacts of aerosols on short-range weather forecasts

S. R. Kolusu et al.

Title Page

Abstract

Introduction

Conclusions

References

Tables

Figures



Back

Close

Full Screen / Esc

Printer-friendly Version

Interactive Discussion



- van der Werf, G. R., Randerson, J. T., Giglio, L., Collatz, G. J., Mu, M., Kasibhatla, P. S., Morton, D. C., DeFries, R. S., Jin, Y., and van Leeuwen, T. T.: Global fire emissions and the contribution of deforestation, savanna, forest, agricultural, and peat fires (1997–2009), *Atmos. Chem. Phys.*, 10, 11707–11735, doi:10.5194/acp-10-11707-2010, 2010. 18886
- 5 Ward, D. S., Kloster, S., Mahowald, N. M., Rogers, B. M., Randerson, J. T., and Hess, P. G.: The changing radiative forcing of fires: global model estimates for past, present and future, *Atmos. Chem. Phys.*, 12, 10857–10886, doi:10.5194/acp-12-10857-2012, 2012. 18889
- Wilson, D. R. and Ballard, S. P.: A microphysically based precipitation scheme for the UK Meteorological Office Unified Model, *Q. J. Roy. Meteor. Soc.*, 125, 1607–1636, 1999. 18888
- 10 Wu, L., Su, H., and Jiang, J. H.: Regional simulations of deep convection and biomass burning over South America: 2. Biomass burning aerosol effects on clouds and precipitation, *J. Geophys. Res.-Atmos.*, 116, D17209, doi:10.1029/2011JD016106, 2011. 18886, 18895, 18899
- Yu, H., Liu, S., and Dickinson, R.: Radiative effects of aerosols on the evolution of the atmospheric boundary layer, *J. Geophys. Res.-Atmos.*, 107, 4142, doi:10.1029/2001JD000754, 15 2002. 18885
- Zhang, Y., Fu, R., Yu, H., Dickinson, R. E., Juarez, R. N., Chin, M., and Wang, H.: A regional climate model study of how biomass burning aerosol impacts land-atmosphere interactions over the Amazon, *J. Geophys. Res.-Atmos.*, 113, D14S15, doi:10.1029/2007JD009449, 2008. 18886
- 20 Zhang, Y., Fu, R., Yu, H., Qian, Y., Dickinson, R., Silva Dias, M. A. F., da Silva Dias, P. L., and Fernandes, K.: Impact of biomass burning aerosol on the monsoon circulation transition over Amazonia, *Geophys. Res. Lett.*, 36, L10814, doi:10.1029/2009GL037180, 2009. 18886

Impacts of aerosols on short-range weather forecasts

S. R. Kolusu et al.

Title Page

Abstract

Introduction

Conclusions

References

Tables

Figures



Back

Close

Full Screen / Esc

Printer-friendly Version

Interactive Discussion



Table 1. Experimental setups using the MetUM model.

Experiment set up	Aerosol Representation
NOA	No Aerosol
CLIM	Direct radiative effect (DRE) from climatological BBA
PROG	DRE from CLASSIC BBA prognostic scheme

Impacts of aerosols on short-range weather forecasts

S. R. Kolusu et al.

Title Page

Abstract

Introduction

Conclusions

References

Tables

Figures



Back

Close

Full Screen / Esc

Printer-friendly Version

Interactive Discussion

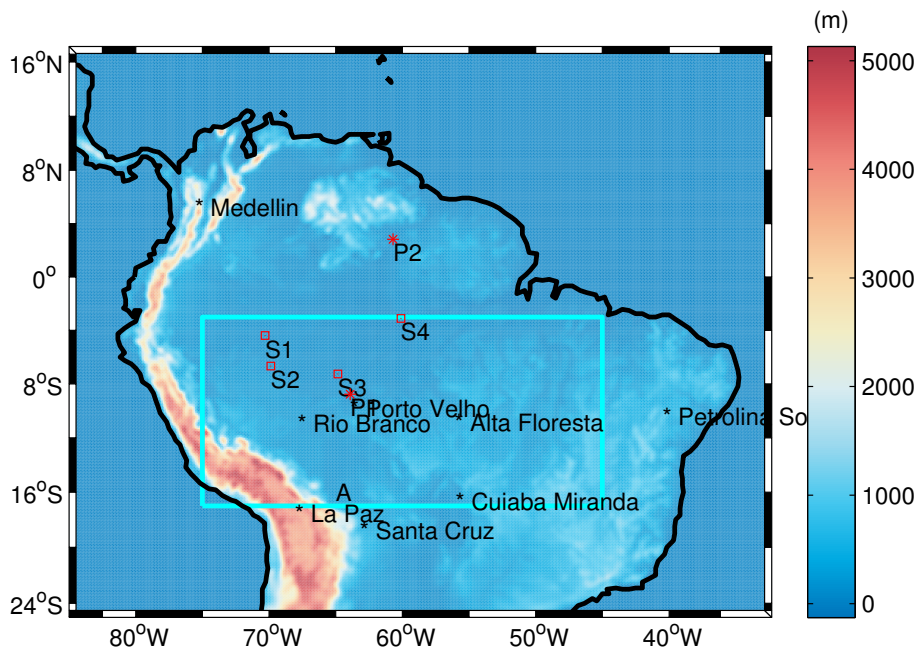


Figure 1. Model domain and orography. Box A (blue) is used to calculate the short-range weather changes due to BBA in Table 2. S1, S2, S3, S4 show locations of surface observations at Benjamin Constant, Eirunepe, Labrea and Manaus, respectively. P1 and P2 are locations of radiosoundings at Porto Velho and Boa Vista. Black asterisks (*) denote AERONET stations.

Impacts of aerosols
on short-range
weather forecasts

S. R. Kolusu et al.

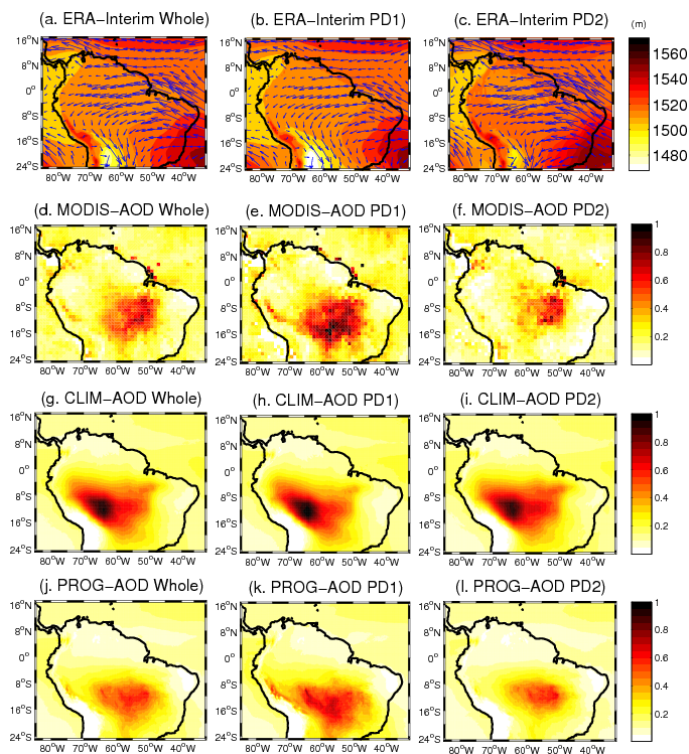


Figure 2. Geopotential height and wind vectors at 850 hPa from ERA-Interim (a, b, c) and 550 nm AODs from MODIS (d, e, f), from total AOD in CLIM (g, h, i) and total AOD in PROG (j, k, l). Plots are for whole period (a, d, g, j), first period PD1 (b, e, h, k), second period PD2 (c, f, i, l).

Impacts of aerosols on short-range weather forecasts

S. R. Kolusu et al.

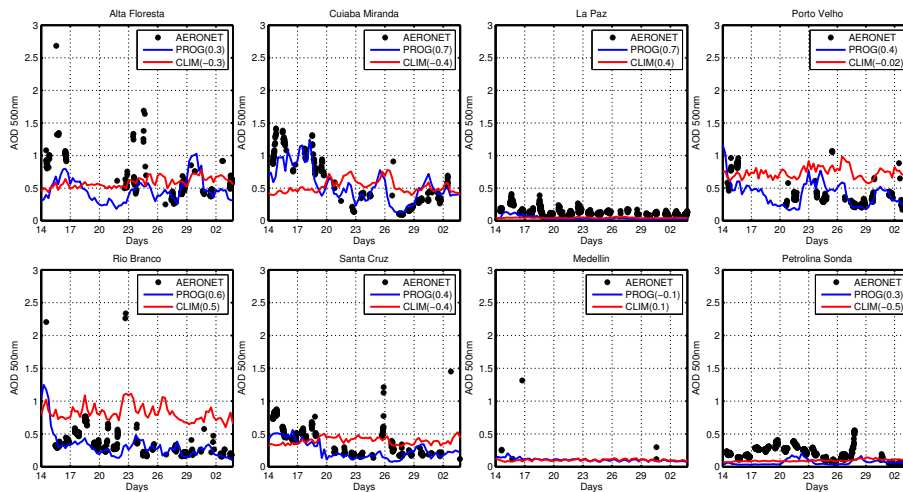


Figure 3. Time series AERONET (black *), PROG (blue line), CLIM (red line) 550 nm AOD at different locations. Correlation coefficients between AERONET and models are shown in parenthesis.

Title Page

Abstract

Introduction

Conclusions

References

Tables

Figures



Back

Close

Full Screen / Esc

Printer-friendly Version

Interactive Discussion



Impacts of aerosols
on short-range
weather forecasts

S. R. Kolusu et al.

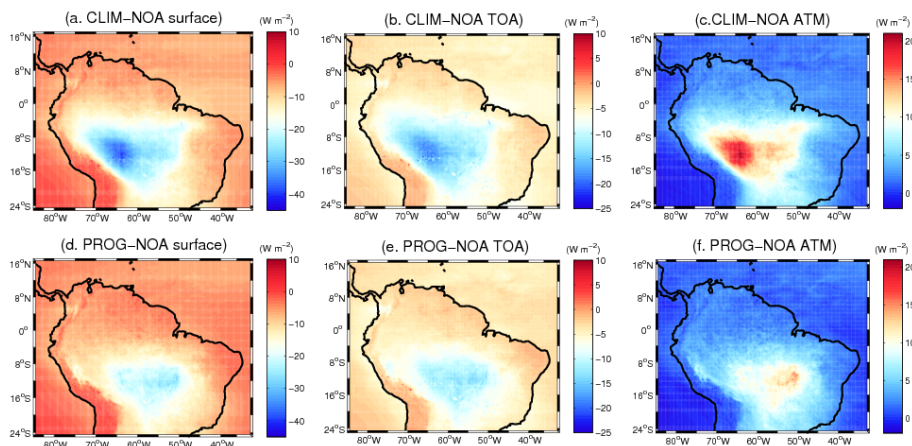


Figure 4. Impact of (top row) CLIM and (bottom row) PROG aerosol representations on **(a, d)** the net surface radiation, **(b, e)** net TOA radiation, **(c, f)** net atmospheric divergence averaged over the whole SAMBBA period for clear-sky.

[Title Page](#)[Abstract](#)[Introduction](#)[Conclusions](#)[References](#)[Tables](#)[Figures](#)[Back](#)[Close](#)[Full Screen / Esc](#)[Printer-friendly Version](#)[Interactive Discussion](#)

Impacts of aerosols
on short-range
weather forecasts

S. R. Kolusu et al.

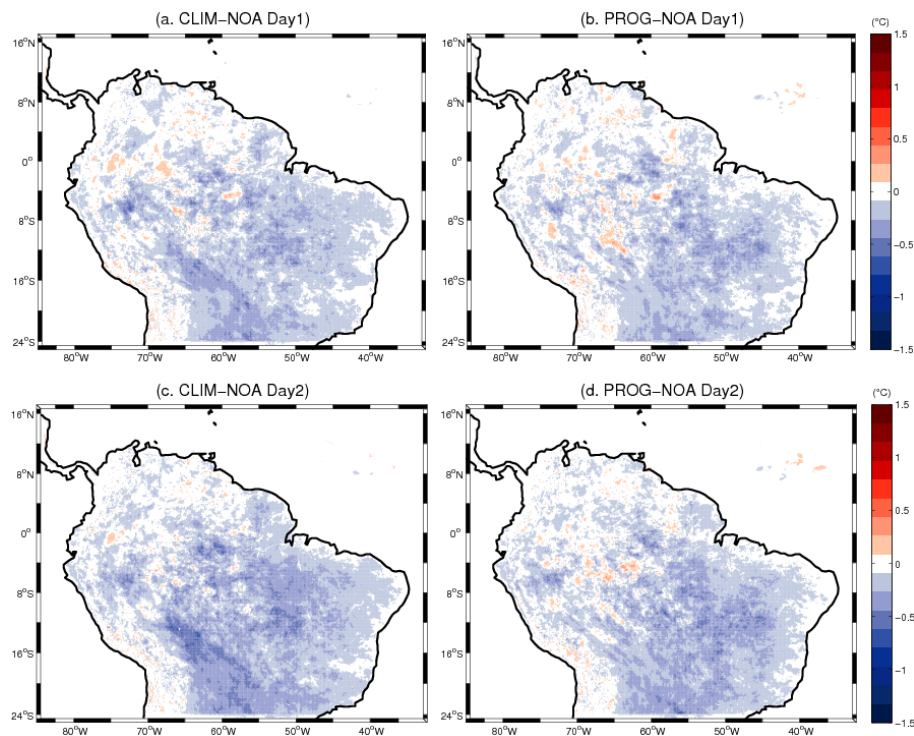


Figure 5. Impact of BBA on 2 m air temperature for day 1 (a, b) and day 2 (c, d).

[Title Page](#)[Abstract](#)[Introduction](#)[Conclusions](#)[References](#)[Tables](#)[Figures](#)[Back](#)[Close](#)[Full Screen / Esc](#)[Printer-friendly Version](#)[Interactive Discussion](#)

Impacts of aerosols
on short-range
weather forecasts

S. R. Kolusu et al.

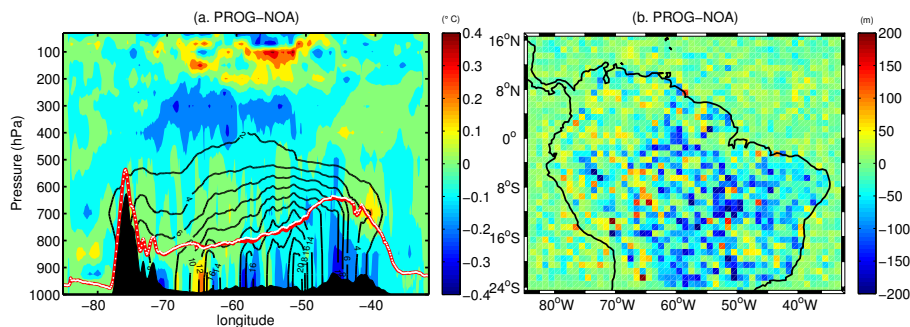


Figure 6. (a) Differences in potential temperature (coloured), BBA mass mixing ratio (ng g^{-1} , black contours) averaged over 10–13° S for the entire campaign period at 18:00 UTC for PROG-NOA. Red and white lines are boundary layer depth of PROG and NOA respectively. Topography is masked black. (b) Differences in BL height PROG-NOA.

[Title Page](#)[Abstract](#)[Introduction](#)[Conclusions](#)[References](#)[Tables](#)[Figures](#)[◀](#)[▶](#)[◀](#)[▶](#)[Back](#)[Close](#)[Full Screen / Esc](#)[Printer-friendly Version](#)[Interactive Discussion](#)

Impacts of aerosols
on short-range
weather forecasts

S. R. Kolusu et al.

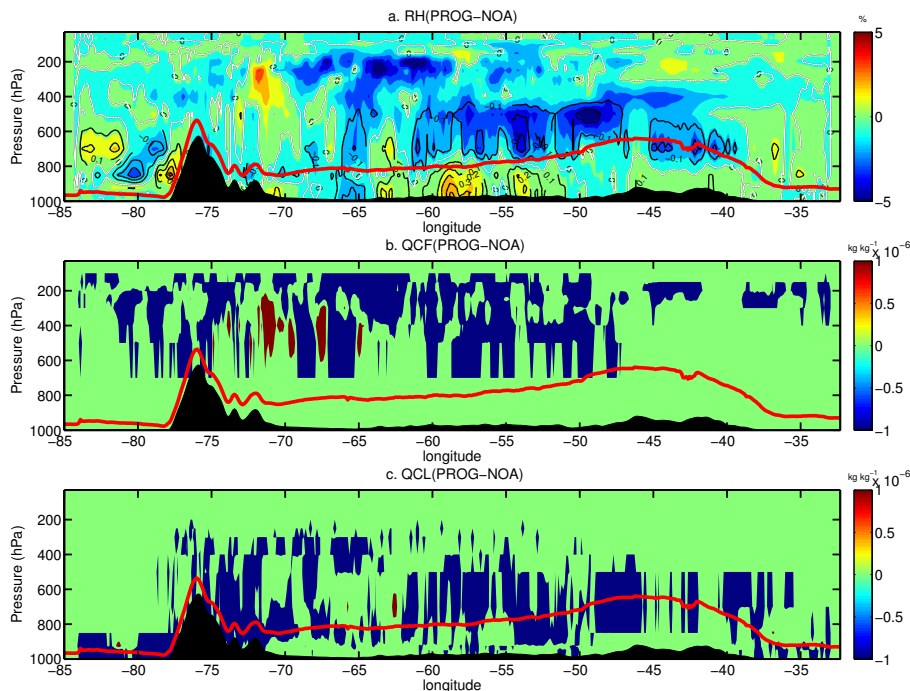


Figure 7. As Fig. 6 but differences are for **(a)** Relative humidity (coloured), black contours are specific humidity (g kg^{-1}), **(b)** Ice cloud water (QCF), **(c)** Liquid cloud water (QCL). Red line is boundary layer depth of PROG. Topography is masked in black.

Title Page

Abstract

Introduction

Conclusions

References

Tables

Figures

◀

▶

◀

▶

Back

Close

Full Screen / Esc

Printer-friendly Version

Interactive Discussion



Impacts of aerosols
on short-range
weather forecasts

S. R. Kolusu et al.

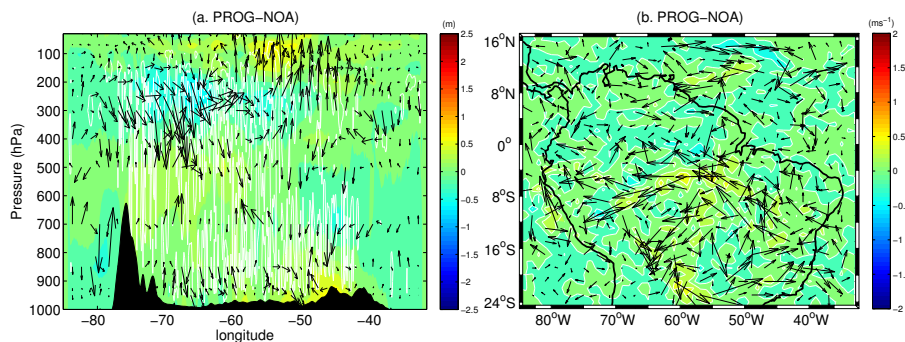


Figure 8. (a) Differences in geopotential height (coloured) and u, v winds (arrows) averaged over 10–13° S for the SAMBBA whole period, for PROG-NOA, white contours show differences in vertical wind. Black masked area is the topography. (b) Circulation and wind speed changes at 700 hPa for PROG-NOA.

[Title Page](#)[Abstract](#)[Introduction](#)[Conclusions](#)[References](#)[Tables](#)[Figures](#)[Back](#)[Close](#)[Full Screen / Esc](#)[Printer-friendly Version](#)[Interactive Discussion](#)

Impacts of aerosols on short-range weather forecasts

S. R. Kolusu et al.

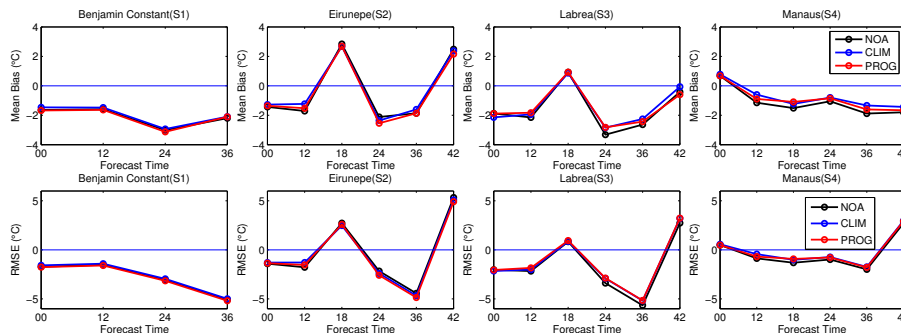


Figure 9. Mean bias and RMS error of modelled temperature at S1, S2, S3 and S4 locations (Fig. 1), averaged over the whole period.

Title Page

Abstract

Introduction

Conclusions

References

Tables

Figures

⏪

⏩

◀

▶

Back

Close

Full Screen / Esc

Printer-friendly Version

Interactive Discussion



Impacts of aerosols
on short-range
weather forecasts

S. R. Kolusu et al.

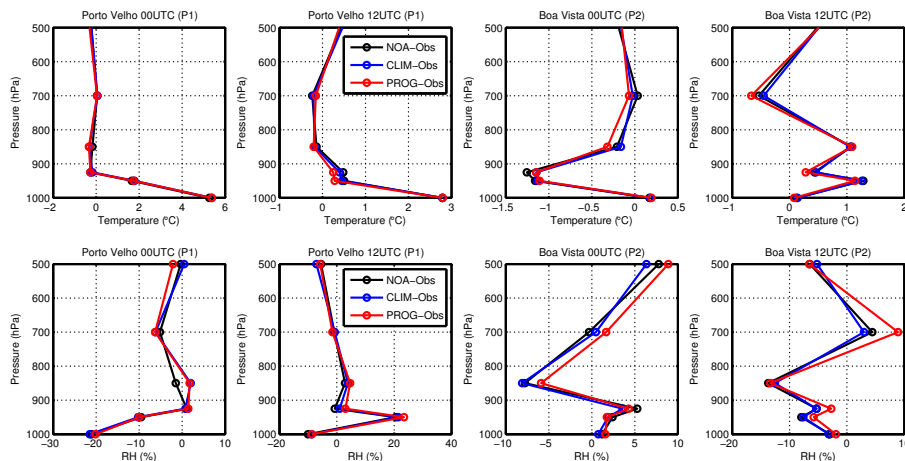


Figure 10. Profiles of modelled minus observed temperature and relative humidities from radiosondes at P1 and P2 (locations shown in Fig. 1).

Title Page

Abstract

Introduction

Conclusions

References

Tables

Figures



Back

Close

Full Screen / Esc

Printer-friendly Version

Interactive Discussion



Impacts of aerosols on short-range weather forecasts

S. R. Kolusu et al.

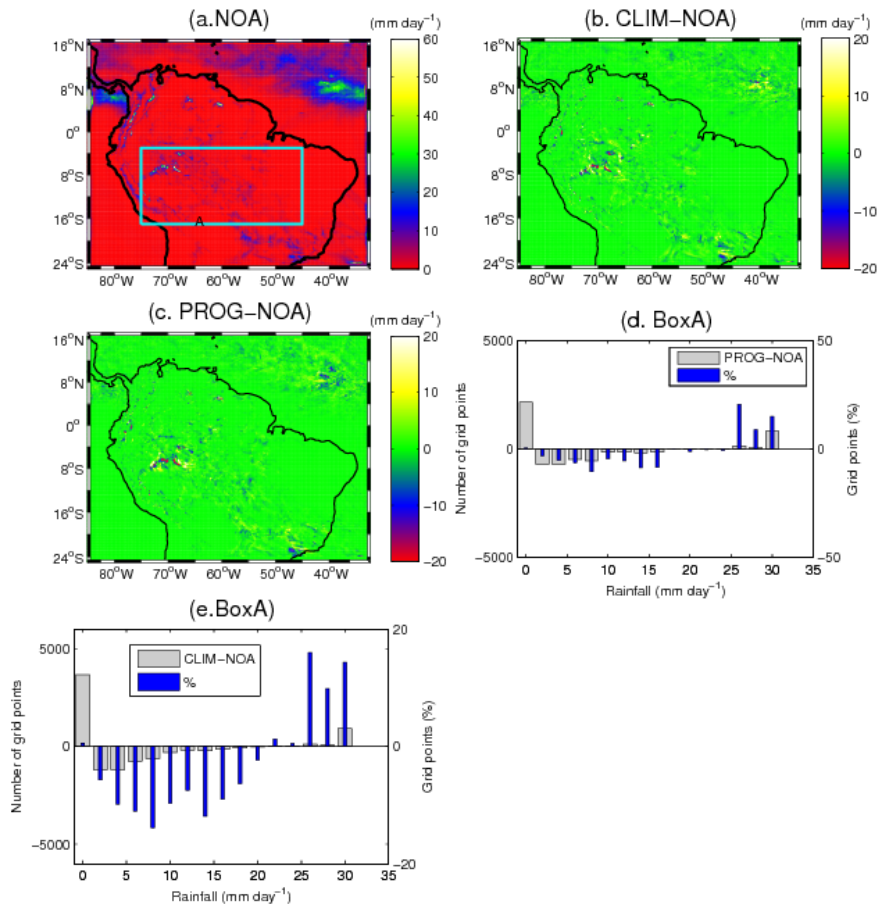


Figure 11. The whole SAMBBA period mean rainfall (a), differences in rainfall (b, c) and changes to frequency distributions of precipitation (d–e) from BBA to NOA for box A. Blue bars are in percentage with respect to differences.

Title Page

Abstract Introduction

Conclusions References

Tables Figures

◀ ▶

◀ ▶

Back Close

Full Screen / Esc

Printer-friendly Version

Interactive Discussion

